Sensors & Actuators: B. Chemical 328 (2021) 128955

Contents lists available at ScienceDirect

Sensors and Actuators: B. Chemical

journal homepage: www.elsevier.com/locate/snb

Improving selectivity of ion-sensitive membrane by polyethylene glycol doping

Qitao Hu [a], Si Chen [a], Zhenqiang Wang [b], Zhen Zhang [a,*]

[a] Division of Solid-State Electronics, Department of Electrical Engineering, The Ångström Laboratory, Uppsala University, P.O. Box 534, SE-75121 Uppsala, Sweden
[b] Department of Chemistry, The University of South Dakota, Churchill-Haines Laboratories, Room 115, 414 East Clark Street, Vermillion, SD 57069-2390, United States

ARTICLE INFO

Keywords:
Ion selectivity
Polyethylene glycol
Mixed-matrix membrane
Ion-selective field-effect transistor
Silicon nanowire
Multiplexed detection

ABSTRACT

Hydrophobic ions can generate considerable interference to ion detection in a complex analyte with membrane-based ion-selective sensors, due to the hydrophobic interaction. In this paper, we demonstrate that the interference from the hydrophobic interaction to the sensors can be significantly reduced by incorporating hydrophilic polyethylene glycol (PEG) into the membrane. The sensor is a silicon nanowire field-effect transistor (SiNWFET) with its surface functionalized with an ionophore-doped mixed-matrix membrane (MMM), where the ionophore is either a commercial Na-ionophore III or a novel synthetic metal-organic supercontainer. The incorporation of PEG suppresses the partitioning of hydrophobic ions into the MMM and thus reduces their interference to the detection of target ions. This is evidenced with an improvement in selectivity for Na^+ detection in the presence of interfering methylene blue (MB^+) ion by more than an order of magnitude. It further enables detection of Na^+ and MB^+ using a SiNWFET sensor array in a multiplexed manner with controlled susceptivity to cross-interference and a greatly expanded dynamic range.

1. Introduction

Ion detection in liquid samples, such as river water, sweat, and serum, plays an important role in environmental monitoring, disease diagnosis, and medical analysis [1–4]. Multiplexed detection with sensors integrated on a single chip can simultaneously detect multiple target ions and acquire comprehensive and complementary information of the analyte in a timely manner [4,5]. However, a real-world liquid sample usually contains complex components such as elemental ions, molecular ions, and biomolecules. These complex components may interfere with ion sensors by generating non-specific and false responses and cause selectivity issue [5–7].

Silicon nanowire field-eff ;ect transistor (SiNWFET) [8] has attracted a great deal of attention in chemical sensing [9,10], label-free biosensing [11,12], and gas sensing [13] due to its high charge sensitivity and possibility of high-density integration. SiNWFET based ion-selective sensors (SiNW-ISFETs) can be realized by functionalizing the sensor surface with an ionophore-incorporated mixed-matrix membrane (MMM). This membrane based sensors have been widely used for detection of elemental ions [14] and molecular ions [5,15]. The ionophore has to be designed with high binding affinity and selectivity towards a target ion. Variation of the target ion activity in the liquid sample will lead to a change of the MMM/sample interfacial potential therefore a shift in the threshold voltage (V_{TH}) of the SiNW-ISFET. MMM can be drop-casted onto the chip surface [16] and has been shown to be more reliable for a stable interfacial potential formation than covalently functionalized ion receptors [17].

However, MMM itself also has a high affinity towards hydrophobic molecules and ions owing to its hydrophobic nature. As a result, organic molecules and molecular ions in the liquid sample can partition into the MMM and generate non-specific signal. In our previous work [5], we have demonstrated that such partitioning can adversely affect the sensor performance, particularly in ion detection with the presence of molecular ions. Specifically, the presence of a molecular ion, *i.e.*, methylene blue (MB^+), in the liquid sample can considerably limit the sensitivity of the Na^+ SiNW-ISFET sensor (Na^+-sensor). MB^+ activity (a_{MB^+}) changes in the liquid sample also generate false responses to the Na^+-sensor. Consequently, multiplexed detection of Na^+ and MB^+ ions was demonstrated only in a limited a_{MB^+} range, *i.e.*, between 1 μM and 7 μM. MB^+ was selected as a representative interfering ion in our study due to its known hydrophobicity and environmental implications.

It has been proved that polyethylene glycol (PEG) incorporation

* Corresponding author.
E-mail address: zhen.zhang@angstrom.uu.se (Z. Zhang).

https://doi.org/10.1016/j.snb.2020.128955
Received 18 May 2020; Received in revised form 21 September 2020; Accepted 22 September 2020
Available online 28 September 2020

could reduce the hydrophobicity of a membrane [18,19]. Therefore we expect that incorporating PEG to the MMM can lower its affinity to hydrophobic ions and benefit the sensor selectivity. In this work, we demonstrate that the interference from hydrophobic interactions can indeed be significantly reduced by incorporating hydrophilic PEG into the MMM. The PEG incorporation greatly improved the selectivity of the Na^+-sensor against hydrophobic ions, *e.g.*, MB^+. The effect of PEG doping on the selectivity is also quantitatively examined. In the end, multiplexed detection of Na^+ and MB^+ ions with a widened range is achieved in a single liquid sample with the improved MMM.

2. Material and methods

2.1. Reagents and materials

High molecular weight poly(vinylchloride) (PVC), PEG 3350, Na-ionophore III, Tetrahydrofuran (THF), Bis(2-ethylhexyl)sebacate (DOS), potassium tetrakis(4-chlorophenyl) borate (KTpClPB), KCl, and NaCl were purchased from Sigma-Aldrich and used without any further purification. HCl was purchased from BASF and methylene blue from Merck Millipore. The metal-organic supercontainer (MOSC) based ionophore (designated as **1-Co**) was synthesized following a published procedure [20]. A schematic of MOSC **1-Co** structure is shown in Fig. 1a. All activity series were prepared using deionized (DI) water (18.2 MΩ cm).

2.2. Device fabrication

The SiNW-ISFETs were fabricated on silicon-on-insulator (SOI) substrates by means of standard silicon process. The SOI wafers comprised a 260-nm-thick lightly p-type doped silicon layer on top of a 375-nm-thick buried oxide (BOX). Details regarding the process can be found in our published paper [21]. In brief, the silicon layer in the channel region was thinned down from 260 to 40 nm via thermal oxidation. The SiNW channel was defined by lithography and dry etching and was then laterally shrunk to the desired width. To reduce the series resistance, PtSi/p^+-Si leads were used for connecting the SiNW-ISFETs to the contact pads placed at the edges of the chip. Finally, a fresh thin silicon oxide (SiO_2) film was grown via rapid thermal oxidation to serve as gate insulator and passivation on the chip. A top-view SEM image of a SiNW-ISFET is shown in Fig. 1b.

2.3. Preparation of MMMs

Five types of MMMs were prepared: Na-ionophore III incorporated MMM without PEG (Na^+-MMM-control), with 10 %, 20 %, and 30 % PEG (w/w) (Na^+-MMM-10 %, Na^+-MMM-20 %, and Na^+-MMM-30 %), and MOSC **1-Co** incorporated MMM (MB^+-MMM). Detailed compositions for the MMMs are listed in Table 1. The preparation procedure for MB^+-MMM can be found in our previous work [15], while that of Na^+-MMMs is available in the literature [22].

Prior to sensor functionalization, the MMM solutions were stirred for 10 min until it became homogeneous. To functionalize the SiNW-ISFETs, 5 μL of MMM solution were drop-casted on the device area by pipetting (Fig. 1c). Ion-selective electrodes (ISEs) were fabricated by dipping pipette tips into the MMM solutions, allowing ~10 μL solution to fill the pipette tips by capillary force [15]. Subsequently, Ag/AgCl pellets were inserted into the pipette body. Saturated KCl solution was then injected into the body to complete ISEs fabrication. Before any measurement was performed, the Na^+-sensors were conditioned in a 100 mM NaCl solution for 4 h and MB^+-sensors in a 10 μM MB solution for 10 h.

2.4. Electrical characterizations

All electrical measurements were performed at room temperature. Transfer characteristics (I_{DS} vs. V_G) and real-time current of the SiNW-ISFETs were measured on a probe-station using a Keysight B1500A precision semiconductor parameter analyzer. As schematically illustrated in Fig. 1d, a polydimethylsiloxane (PDMS) container was utilized to hold the liquid sample during the measurement. A reference electrode (Ag/AgCl, Harvard Apparatus) was immersed in the liquid sample to apply a gate voltage (V_G). During sensing, the SiNW-ISFET sensors were

Table 1
Compositions of Na^+-MMMs and MB^+-MMM prepared in this study.

Composition	Na^+-MMM-control	Na^+-MMM-10%	Na^+-MMM-20%	Na^+-MMM-30%	MB^+-MMM
Na-ionophore III	10 mg	10 mg	10 mg	10 mg	
MOSC **1-Co**					25.7 mg
KTpClPB	4.5 mg	4.5 mg	4.5 mg	4.5 mg	5.0 mg
PVC	165 mg	165 mg	165 mg	165 mg	330 mg
THF	5 mL	5 mL	5 mL	5 mL	5 mL
DOS	361 μL	361 μL	361 μL	361 μL	722 μL
MB					3.2 mg
PEG		16 mg	32 mg	48 mg	

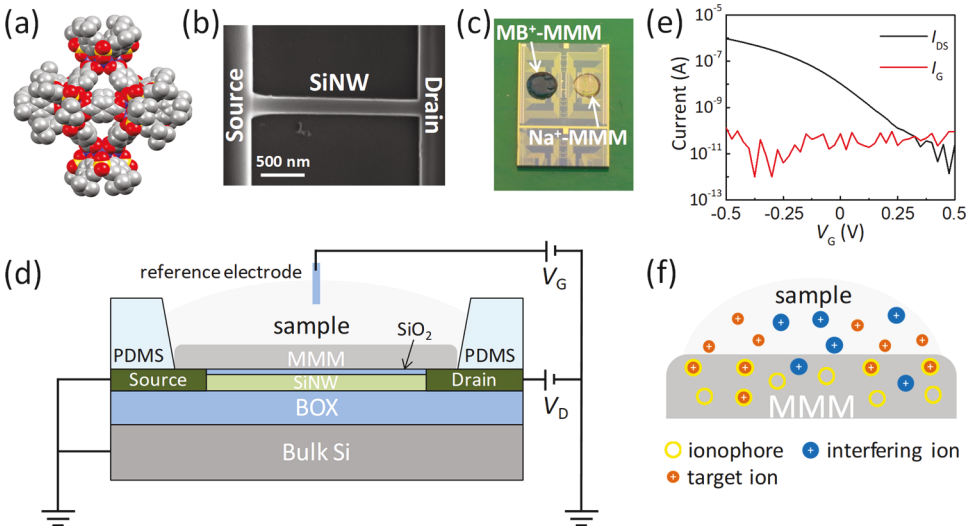

Fig. 1. (a) Structural representation of the MOSC **1-Co**, where the gray, yellow, red, and blue sphere refers to C, S, O, and Co atom, respectively, (b) Top-view SEM image of a SiNW-ISFET with a SiNW channel width of 180 nm, (c) optical image of a SiNW-ISFET chip functionalized with Na^+- and MB^+-MMMs, (d) schematic representation of the cross-section of a SiNW-ISFET as well as the measurement arrangement for ion sensing, (e) transfer characteristics of a MMM-functionalized SiNW-ISFET measured in 1 mM KCl, and (f) schematic illustration of the charge separation and equilibrium at the MMM/sample interface.

biased in their subthreshold region with a constant drain-to-source voltage (V_{DS} = 1 V). The solution exchanges were realized manually using a pipette. Electrode potential (E_{WE}) of the ISE was measured on a VSP 300 (Bio-Logic, France) electrochemical workstation with a conventional 3-electrode configuration.

3. Results and discussion

3.1. Characterization of SiNW-ISFET

I_{DS} vs. V_G curve of an MMM-functionalized SiNW-ISFET is shown in Fig. 1e. The SiNW-ISFET exhibits a subthreshold slope (*SS*) of 124 mV/dec and an on-to-off current ratio (I_{on}/I_{off}) of ~10^5. The gate leakage current (I_G) of the SiNW-ISFET is below 10^{-10} A, and is more than two orders of magnitude lower than the I_{DS} of the SiNW-ISFET during sensing. As schematically illustrated in Fig. 1d, when the electrical potential of the liquid sample is fixed by a reference electrode, any change in the MMM/sample phase boundary potential (E_{PB}) will lead to a corresponding shift in the threshold voltage (V_{TH}) of the SiNW-ISFET [5]. Fig. 1f is a zoomed-in view of the MMM/sample interface. The ionophores in the surface of the MMM can specifically capture the target ions [15], while the hydrophobic interfering ions can also partition into the MMM due to the hydrophobic nature of the MMM. In the presence of both target (Na^+) and interfering (MB^+) ions, the E_{PB} at the MMM/sample interface can be expressed as [23]

$$E_{PB} = E^0_{PB} + \frac{RT}{zF}\ln(a_{Na^+} + K_{Na,MB}a_{MB^+}) \quad (1)$$

where E^0_{PB} is the phase boundary constant, R the universal gas constant, T the temperature, z the valency of target and interference ions, F the Faraday constant, a_{Na^+} and a_{MB^+} the ion activities of target and interfering ions, respectively, and $K_{Na,MB}$ the selectivity coefficient. $K_{Na,MB}$ reflects the difference in the affinities of the MMM towards Na^+ and MB^+ ions. An MMM with lower affinity to MB^+ ion will have a smaller value of $K_{Na,MB}$, resulting in the Na^+ sensing less vulnerable to the interfering MB^+ ion.

3.2. Effects of PEG doping

THF solutions of MMM without PEG and MMMs with 10 % and 20 % of PEG are transparent as seen in Fig. 2a. The solution with 30 % of PEG is however turbid with visible particles because PEG are not completely dissolved in THF. The four Na^+-MMMs were conditioned in a 100 μM MB^+ solution for 10 min to test the partitioning of MB^+ ions into the Na^+-MMMs. As shown in Fig. 2b, the PEG-doped Na^+-MMMs all exhibit a light blue color in comparison to a much darker blue color observed in the control, *i.e.*, the Na^+-MMM without PEG doping. Evidently, PEG can thermodynamically impede the partitioning process owing to its hydrophilicity, which makes the Na^+-MMMs less hydrophobic thus having lower affinity to the hydrophobic MB^+ ions.

The effect of PEG doping on MB^+ partitioning is further examined by measuring the E_{WE} of the ISEs produced with the Na^+-MMMs in liquid with a constant a_{MB^+} = 10 μM. Since ISEs are fabricated with internal aqueous solution, *i.e.*, saturated KCl solution (see the inset of Fig. 2c), the value of E_{WE} is independent of the standard chemical potential of membrane and only depends on the ratio of a_{MB^+} in the aqueous and membrane phases, which can be a quantitative measure of the amount of MB^+ ions partitioned into the Na^+-MMM [15,23]. As shown in Fig. 2c, E_{WE} becomes more negative with increasing PEG concentration in the Na^+-MMM. Specifically, E_{WE} is lowered by ~60 mV with 10 % of PEG doping, which can be converted to ~10× reduction of a_{MB^+} in the Na^+-MMM. Further increase of PEG concentration beyond 10 % shows less significant effect on E_{WE}, which is consistent with the observed color differences of the Na^+-MMMs as shown in Fig. 2b. The Gibbs free energy change (ΔG) of MB^+ partitioning into membranes is calculated using the measured E_{WE} with the method in a published paper [24]. The results are noted in Fig. 2c. The negative calculated ΔG indicates that MB^+ has a trend to partition into membrane. The ΔG value increases with higher PEG doping concentration, which means that PEG doping is capable to suppress the MB^+ partitioning.

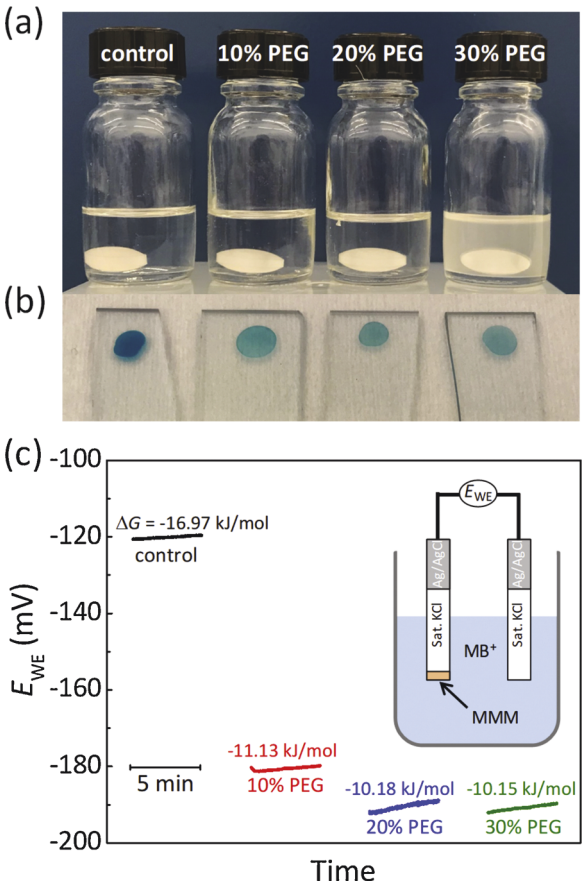

Fig. 2. Images of (a) Na^+-MMM THF solutions with different PEG concentrations and (b) Na^+-MMMs on glasses after conditioning in a 100 μM MB^+ solution for 10 min. (c) E_{WE} of ISEs fabricated with Na^+-MMMs measured in a 10 μM MB^+ solution. The calculated ΔG values of MB^+ partitioning into different membranes are also noted. The E_{WE} was recorded for 5 min for each ISE to check the ISE stability. Inset: schematic of E_{WE} measurement arrangement.

3.3. Na^+ ISFET sensors

The selectivities of Na^+-sensors are characterized by measuring their responses to interfering ions (MB^+). Fig. 3a depicts the V_{TH} shift (ΔV_{TH}) versus a_{MB^+} for different Na^+-sensors. Hereafter, Na^+-sensors functionalized with Na^+-MMM-control, Na^+-MMM-10 %, Na^+-MMM-20 %, and Na^+-MMM-30 % will be referred as Na-control, Na-10, Na-20, and Na-30, respectively. The measurements were conducted in a 1 mM NaCl background electrolyte to maintain a constant ionic strength of the primary ion. The Na^+-sensor with higher PEG doping in the MMM shows lower responses to the increased a_{MB^+}. To extract the selectivity coefficient $K_{Na,\,MB}$, response curves in Fig. 3a are fitted with Eq. (1) The fitting curves are shown as dashed lines in Fig. 3a and the extracted $K_{Na,\,MB}$ are summarized in Table 2. PEG incorporation clearly improves the selectivity of the Na^+-MMMs against the hydrophobic molecular ions, *i.e.*, MB^+, as evidenced by the reduction in $K_{Na,\,MB}$. In particular, $K_{Na,\,MB}$ for Na-20 and Na-30 is reduced by more than an order of magnitude in comparison to that of the Na-control.

Na^+ sensing with the Na^+-sensors is conducted to evaluate possible adverse effect of PEG doping. Fig. 3b plots ΔV_{TH} versus a_{Na^+} for different Na^+-sensors. The response curves of Na-control, Na-10, and Na-20

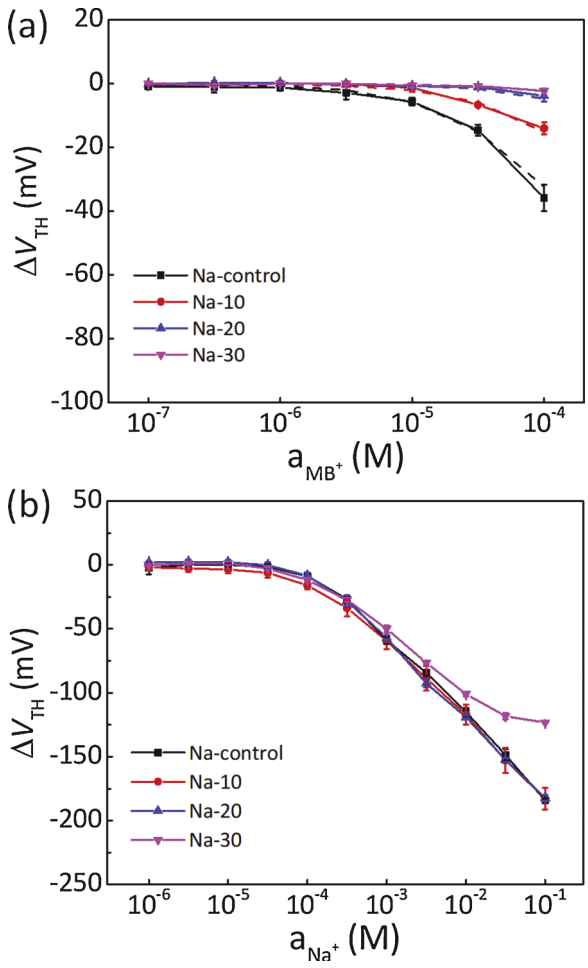

Fig. 3. ΔV_{TH} versus (a) a_{MB^+} in 1 mM NaCl and (b) a_{Na^+} in 1 mM KCl for different Na^+-sensors. In (a), solid and dashed lines represent measured and fitting results, respectively.

Table 2
Extracted $K_{Na,\ MB}$ for different Na^+-MMMs.

MMM	Na^+-MMM-control	Na^+-MMM-10%	Na^+-MMM-20%	Na^+-MMM-30%
$K_{Na,\ MB}$	25	8	2	0.9

basically overlap, showing a near-ideal sensitivity of 60 mV/decade of a_{Na^+} and a lower detection limit of ~ 60 μM. The results demonstrate that PEG doping has negligible adverse effects on Na^+ detection for Na-10 and Na-20. However, further increase of PEG doping in the Na^+-MMM may lead to deterioration in sensing performance, particularly in the high a_{Na^+} region, as revealed by the response curve of Na-30. The significant deviation from Nernstian response for the Na-30 when a_{Na^+} is above 10 mM arises from the co-extraction of Na^+ and Cl^- ions from the liquid sample into the MMM, leading to the so-called Donnan failure [23]. The co-extraction process will likely be enhanced by the presence of PEG in the MMM due to the reduced hydrophobicity which facilitates the extraction of Cl^- ions into MMM. Such issue can be mitigated by further optimization of the MMM composition, *e.g.*, ionophore to ionic site ratio [23].

Further, a series of experiments are conducted to exam the effects of PEG doping on the selectivity to K^+, detection limit, and reversibility of Na^+ sensors. In Figure S1a, the responses of Na-control, Na-10, Na-20, and Na-30 to Na^+ and K^+ are measured. The detection limits of Na^+ for different Na^+ sensors extracted from Figure S1a are listed in Table S1. Table S2 lists the selectivity coefficients to K^+ for Na^+ sensors extracted from Figure S1a with the method in our previous work [5]. The results suggest that PEG doping has insignificant effect on the performance of the Na^+ sensors in terms of selectivity to K^+ and detection limit. The reversibility data of Na^+ sensors is presented in Figure S2a, where the Na^+ activity is switched between 100 μM and 300 μM repeatedly with 1 mM KCl background solution. The Na^+ sensors show reversible responses of ~ 22 mV, which is in good agreement with their sensitivities as shown in Fig. 3a. To verify the stability of PEG in Na^+-MMM, same set of measurements were conducted again after the Na^+ sensors have been stored in 10 nM NaCl solution for 5 days. The results are presented in Figure S1b, Table S1, Table S2, and Figure S2b. The performances of the Na^+ sensors are quite stable within 5 days, which confirms that the extrusion effect of PEG from membrane is negligible.

3.4. Multiplexed analysis

Finally, multiplexed detection of MB^+ and Na^+ ions in a single liquid sample is conducted, using the Na^+-sensor with improved selectivity. The MB^+- and Na^+-sensors are integrated on the same chip by manually drop-casting two MMMs onto the sensors. In current experiment, Na-20 is selected as the Na^+-sensor. As shown in Fig. 4, a_{MB^+} in the liquid sample is first increased from 1 to 10 μM and then from 10 to 100 μM while a_{Na^+} is 100 μM and remains the same. Correspondingly, the MB^+-sensor shows ΔV_{TH} of 65.3 and 52.3 mV while the responses of the Na^+-sensor are negligible. The sensitivity of the MB^+-sensor based on MOSC **1-Co** is in good agreement with our previously reported results [5,15]. Afterwards, a_{Na^+} in the sample is increased from 100 to 300 μM and then from 300 μM to 1 mM, and the corresponding ΔV_{TH} of the Na^+-sensor is 22.7 and 30.5 mV. With these changes, the V_{TH} of the MB^+-sensor remains unaltered. In our previous work, multiplexed detection was performed with a_{MB^+} only up to 7 μM, above which the hydrophobic MB^+ ions will not only generate false response on the Na^+-sensor but also strongly reduce the sensitivity of the Na^+-sensor [5]. The PEG incorporation into the Na^+-MMM clearly suppress such cross-interference and greatly improve the tolerance of the Na^+-sensor to the presence of the MB^+ ion. As a result, the multiplexed detection can be performed in a much wider a_{MB^+} range, *i.e.*, from 1 to 100 μM. It should be noted that the experimental design for the detection of MB^+ and Na^+ ions illustrated in this work is a proof-of-concept demonstration. We anticipate that the demonstrated PEG doping strategy to reduce the interference of hydrophobic interactions to the MMM-based ion sensor will not be limited to the particular ions studied in this work and will be generally applicable in other MMM based sensors.

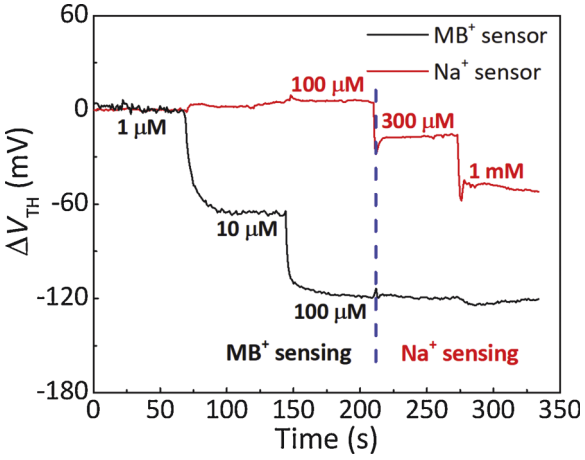

Fig. 4. Multiplexed detection of Na^+ (red) and MB^+ (black) ions in one liquid sample with a background of 1 mM KCl. The MB^+ sensor is functionalized by MB^+-MMM and the Na^+ sensor by Na^+-MMM-20 %.

4. Conclusions

In conclusion, doping PEG to the MMM can reduce its affinity to hydrophobic ions, which leads to much reduced interference from the hydrophobic interactions to the MMM based ion sensor. Such effects are evidenced by significantly improved selectivity of the Na^+-sensors to the MB^+ interference. The improved selectivity of the Na^+-sensor greatly expands the dynamic range in multiplexed detection of molecular (MB^+) and elemental (Na^+) ions in the same liquid sample.

Author contributions

The manuscript was written through contributions of all authors.

Declaration of Competing Interest

The authors declare that they have no known competing financial interests or personal relationships that could have appeared to influence the work reported in this paper.

Acknowledgements

This work was supported by the Swedish Strategic Research Foundation (SSF ICA 12-0047 and FFL15-0174), the Swedish Research Council (VR 2014-5588 and 2019-04690), and the Wallenberg Academy Fellow Program. Z.W. acknowledges the financial support of a National Science Foundation grant (DMR-1709912). Prof. Shi-Li Zhang is acknowledged for comments and support.

Appendix A. Supplementary data

Supplementary material related to this article can be found, in the online version, at doi:https://doi.org/10.1016/j.snb.2020.128955.

References

[1] J. Du, M. Hu, J. Fan, X. Peng, Fluorescent chemodosimeters using “mild” chemical events for the detection of small anions and cations in biological and environmental media, Chem. Soc. Rev. 41 (2012) 4511–4535, https://doi.org/10.1039/C2CS00004K.
[2] C. Jimenez-Jorquera, J. Orozco, A. Baldi, ISFET based microsensors for environmental monitoring, Sensors 10 (2010) 61–83, https://doi.org/10.3390/s100100061.
[3] C.-S. Lee, S.K. Kim, M. Kim, Ion-sensitive field-effect transistor for biological sensing, Sensors 9 (2009) 7111–7131, https://doi.org/10.3390/s90907111.
[4] W. Gao, S. Emaminejad, H. Nyein, S. Challa, K. Chen, A. Peck, H.M. Fahad, H. Ota, H. Shiraki, D. Kiriya, D.-H. Lien, G.A. Brooks, R.W. Davis, A. Javey, Fully integrated wearable sensor arrays for multiplexed in situ perspiration analysis, Nature 529 (2016) 509–514, https://doi.org/10.1038/nature16521.
[5] X. Chen, Q. Hu, S. Chen, N.L. Netzer, Z. Wang, S.-L. Zhang, Z. Zhang, Multiplexed analysis of molecular and elemental ions using nanowire transistor sensors, Sens. Actuators B Chem. 270 (2018) 89–96, https://doi.org/10.1016/j.snb.2018.05.018.
[6] L.M. Bonanno, L.A. DeLouise, Whole blood optical biosensor, Biosens. Bioelectron. 23 (2007) 444–448, https://doi.org/10.1016/j.bios.2007.05.008.
[7] S. Aravamudhan, N.S. Ramgir, S. Bhansali, Electrochemical biosensor for targeted detection in blood using aligned Au nanowires, Sens. Actuators B Chem. 127 (2007) 29–35, https://doi.org/10.1016/j.snb.2007.07.008.
[8] P. Bergveld, Development of an ion-sensitive solid-state device for neurophysiological measurements, IEEE Trans. Biomed. Eng. BM17 (1970) 70–71, https://doi.org/10.1109/TBME.1970.4502688.
[9] S. Chen, J.G. Bomer, E.T. Carlen, A. van den Berg, Al_2O_3/silicon nanoISFET with near ideal nernstian response, Nano Lett. 11 (6) (2011) 2334–2341, https://doi.org/10.1021/nl200623n.
[10] M. Wipf, R.L. Stoop, A. Tarasov, K. Bedner, W. Fu, I.A. Wright, C.J. Martin, E. C. Constable, M. Calame, C. Schönenberger, Selective sodium sensing with gold-coated silicon nanowire field-effect transistors in a differential setup, ACS Nano 7 (7) (2013) 5978–5983, https://doi.org/10.1021/nn401678u.
[11] Y. Cui, Q. Wei, H. Park, C.M. Lieber, Nanowire nanosensors for highly sensitive and selective detection of biological and chemical species, Science 293 (5533) (2001) 1289–1292, https://doi.org/10.1126/science.1062711.
[12] E. Stern, J.F. Klemic, D.A. Routenberg, P.N. Wyrembak, D.B. Turner-Evans, A. D. Hamilton, D.A. LaVan, T.M. Fahmy, M.A. Reed, Label-free immunodetection with CMOS-compatible semiconducting nanowires, Nature 445 (7127) (2007) 519–522, https://doi.org/10.1038/nature05498.
[13] B. Wang, J.C. Cancilla, J.S. Torrecilla, H. Haick, Artificial sensing intelligence with silicon nanowires for ultraselective detection in the gas phase, Nano Lett. 14 (2)) (2014) 933–938, https://doi.org/10.1021/nl404335p.
[14] A. Cao, M. Mescher, D. Bosma, J.H. Klootwijk, E.J.R. Sudhölter, L.C.P.M. de Smet, Ionophore-containing siloprene membranes: direct comparison between conventional ion-selective electrodes and silicon nanowire-based field-effect transistors, Anal. Chem. 87 (2015) 1173–1179, https://doi.org/10.1021/ac504500s.
[15] N.L. Netzer, I. Must, Y. Qiao, S.-L. Zhang, Z. Wang, Z. Zhang, Biomimetic supercontainers for size-selective electrochemical sensing of molecular ions, Sci. Rep. 7 (2017) 45786, https://doi.org/10.1038/srep45786.
[16] L.C.P.M. de Smet, D. Ullien, M. Mescher, E.J.R. Sudhölter, Organic Surface Modification of Silicon Nanowire-based Sensor Devices. Nanowires: Implementations and Applications, Abbass Hashim, InTech, Rijeka Croatia, 2011, pp. 267–288.
[17] P. Bühlmann, L.D. Chen, Ion-Selective Electrodes With Ionophore-doped Sensing Membranes, Supramol Chem, John Wiley & Sons Ltd, 2012.
[18] S. Wongchitphimon, R. Wang, R. Jiraratananon, L. Shi, C.H. Loh, Effect of polyethylene glycol [PEG] as an additive on the fabrication of polyvinylidene fluoride-co-hexafluropropylene [PVDF-HFP] asymmetric microporous hollow fiber membranes, J. Membr. Sci. 369 (2011) 329–338, https://doi.org/10.1016/j.memsci.2010.12.008.
[19] Y.-H. Zhao, B.-K. Zhu, X.-T. Ma, Y.-Y. Xu, Porous membranes modified by hyperbranched polymers: I. Preparation and characterization of PVDF membrane using hyperbranched polyglycerol as additive, J. Membr. Sci. 290 (2007) 222–229, https://doi.org/10.1016/j.memsci.2006.12.037.
[20] N.L. Netzer, F.-R. Dai, Z. Wang, C. Jiang, pH-modulated molecular assemblies and surface properties of metal–organic supercontainers at the air-water interface, Angew. Chem. Int. Ed 53 (2014) 10965–10969, https://doi.org/10.1002/anie.201406733.
[21] S. Chen, S.-L. Zhang, Contacting versus insulated gate electrode for Si nanoribbon field-effect sensors operating in electrolyte, Anal. Chem. 83 (2011) 9546–9551, https://doi.org/10.1021/ac2023316.
[22] J.A. Brunink, J.R. Haak, J.G. Bomer, D.N. Reinhoudt, M.A. McKervey, S.J. Harris, Chemically modified field-effect transistors, a sodium ion selective sensor based on calix [4] arene receptor molecules, Anal. Chim. Acta 254 (1991) 75–80, https://doi.org/10.1016/0003-2670(91)90011-S.
[23] E. Bakker, P. Bühlmann, E. Pretsch, Carrier-based ion-selective electrodes and bulk optodes. 1. General characteristics, Chem. Rev. 97 (1997) 3083–3132, https://doi.org/10.1021/cr940394a.
[24] F. Scholz, R. Gulaboski, K. Caban, The determination of standard Gibbs energies of transfer of cations across the nitrobenzene vertical bar water interface using a three-phase electrode, Electrochem. Commun. 5 (2003) 929–934, https://doi.org/10.1016/j.elecom.2003.09.005.

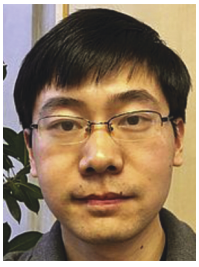

Qitao Hu received the B.S. degree (2015) from University of Science and Technology of China. He is a PhD student at solid-state electronics at Uppsala University in Uppsala, Sweden. His research topic is the ion sensor based on Si nanowire field effect transistors.

Si Chen received the B.S. degree (2004) from University of Science and Technology of China and the M.S. degree (2007) from Shanghai Institute of Ceramics, Chinese Academy of Sciences, and Ph.D. degree (2013) in solid state electronics from Uppsala University, Sweden. He worked as a characterization and development engineer at Solibro Research AB from 2013 to 2016, and joined Uppsala University in 2016 as a researcher. His main research interest is novel device structures and materials for electronic biosensor applications.

Zhenqiang Wang is an associate professor of chemistry at the University of South Dakota, USA. He received his B.S. degree (2000) from Peking University and PhD degree (2006) from the University of South Florida. He did his postdoctoral work at U. C. San Diego before joining the chemistry department at the University of South Dakota. His current research interests include porous materials for selective gas adsorption, supramolecular catalysts that activate small molecules and smart materials that respond to external stimuli.

Zhen Zhang is a professor of solid-state electronics at Uppsala University in Uppsala, Sweden. He received the Ph.D degree in department of microelectronics and information technology from Royal Institute of Technology (KTH) of Sweden in 2008. He worked as a research staff member at IBM T. J. Watson research center at York-town Heights, New York from 2008 to 2013, and joined Uppsala University in 2013. His research interest covers semiconductor based electronic sensors, nanoscale semi-conductor devices and bio-electronics.